coatings

Article

Study of the Geochemical Decay and Environmental Causes of Granite Stone Surfaces in the Built Heritage of Barbanza Peninsula (Galicia, NW Spain)

Ana C. Hernandez [1], Jorge Sanjurjo-Sánchez [1,*] , Carlos Alves [2] and Carlos A. M. Figueiredo [3]

1   Instituto Universitario de Xeoloxía "Isidro Parga Pondal", Edificio Servizos Centrais de Investigación, Universidade da Coruña, Campus de Elviña, 15071 A Coruna, Spain; ana.cristina.hernandez.santome@udc.es
2   LandS/Lab2PT-Landscapes, Heritage and Territory Laboratory (FCT-UIDB/04509/2020), Earth Sciences Department, School of Sciences, University of Minho, 4710-057 Braga, Portugal; casaix@dct.uminho.pt
3   CERENA—Centre for Natural Resources and the Environment, FCT-UIDB/04028/2020, Instituto Superior Técnico, University of Lisbon, 1049-001 Lisbon, Portugal; carlos.m.figueiredo@ist.utl.pt
*   Correspondence: jorge.sanjurjo.sanchez@udc.es

Abstract: In Galicia (NW Spain), granite was the most used stone material in historical buildings. Despite the good properties of granite as a construction material, it overcomes several physical and chemical weathering processes that cause decay, resulting in a loss of value in building materials, architectural elements and details. This is caused by a range of processes, from aesthetic damage to stone erosion. The causes of such decay are well known from case studies of historical buildings, being correlated with atmospheric agents, air pollution and aggregate materials, among others. In this work, we studied 15 historical monuments built with granite blocks of the architectural Heritage of the Barbanza Peninsula (Galicia). Because of the geographic features of this area, there is a steep rainfall and sea spray gradient that allows us to study historical buildings exposed to different environmental conditions in a short distance from the shoreline to inland. We used geochemical, petrological and microscopic tools to assess the decay of the granites and compared the results with environmental factors to assess the role of humidity (rainfall) and sea spray on the decay. Both the observation of coatings and the assessment of weathering have shown that buildings close to the shoreline are more affected by sea salts, while buildings far from the coast are mostly affected by biological weathering. Surprisingly, chemical weathering is higher in a strip area some hundreds of meters away from the sea shore and at lower altitudes (between 10 and 30 m). Indeed, very good correlation is observed for weathering indices, such as CIA, MWPI, VR, Si-Ti index, Kr, CAN and AKN, with a distance to the shoreline from 0.5 km, with linear correlation values ranging from −0.91 to 0.80.

Keywords: weathering; granite; built heritage; decay

1. Introduction

The stone surfaces of historical buildings provide evidence of their past history, stone and the preservation of the architectural and artistic value of building components. Stone, as a building material, is continuously exposed to environmental factors that include water sources (e.g., rainfall, rising groundwater), air pollution and biological colonization, among others [1–6]. All of them can cause several deterioration processes that can result in variable effects: from physical or chemical weathering that results in the erosion of stone surfaces to the development of coatings that enhance the surface preservation [7–10]. In general, such effects include a significant loss of valuable building materials, architectural elements and details, considering aesthetic damage (e.g., discoloration) and the definitive loss of material (e.g., detachment, scaling) [11], as it can be observed in sculptural objects of façades, which are sometimes deficient in the conservation conditions of such materials

through time [3,12,13]. After decades of studies on monuments around the world [11], it is well known that the decay of stone materials is often a complex phenomenon due to a combination of the natural processes of physical, chemical and biological weathering that can act simultaneously over a long time period, meaning that it is necessary to study Heritage buildings from case to case [14–17]. Moreover, while the detachment of stone can be very easily observed by the naked eye, other processes such as chemical weathering are difficult to assess. Chemical weathering can affect to the whole stone block, or stone surfaces, sometimes being involved in the growth of stone coatings, discoloration or color changes, as well as the loss of mechanical strength of stones [5,14,18,19] Indeed, coatings can result from biological growth or other physico-chemical processes, and they have been related to stone decay but also stone preservation due to their possible role in the increase in surface hardness [3,14,18].

Although the effect of some natural environmental factors such as humidity and precipitation or the sea spray effect on stones have been demonstrated [20–22], the existing knowledge about their effects is based on case studies [4,6,15,16]. Because of this, there are no clear statements and quantifications of the effect of such factors. How far onshore does the sea spray have an effect on stone decay in buildings? What is the relationship between the annual precipitation in a geographical area and the effect on chemical weathering in a given rock? So far, it has not been possible to quantify the effect of these environmental factors. Although the answer to these questions is complex, this study is an attempt to provide some answers as the starting point to a deeper study.

In this work, we chose and studied a set of 15 historical monuments built with granite blocks of the architectural Heritage of the Barbanza Peninsula (Galicia, NW Spain). In Galicia, the most historically used stone material for construction purposes is granite, with other stone types, such as schist, gneiss and marble, far less used, as they are less common [23]. Despite the attractive properties of granite (e.g., hardness, low porosity), the granite massifs are exposed to weathering (on a geological timescale), particularly on quarry surfaces [24]. When used as a building material, granite stone blocks are also exposed to weathering agents that increase their deterioration, as occurs with other rock types. It has been demonstrated that such exposure to the environmental factors referred to above usually accelerates the decay at a historical scale period, as observed in other studies in monuments of this region [23–26].

The Barbanza Peninsula is an area off the western coast of Galicia (Figure 1), where granite is the most abundant stone, with this rock being the most widely used in the Heritage monuments in the area [26]. This peninsula is about 416 m^2, with a temperate oceanic climate but with very different average yearly rainfall (from 900 to 3300 mm/year) and humidity, and different exposure to other environments, such as the sea-salt effect, depending on the distance of the buildings to the sea [26]. As there are some small cities with populations around 20 000 inhabitants, the exposure of historical buildings to air pollutants can also be quite different in the area, with this aspect being taken into account in this study.

We took surface granite samples from the selected buildings with the purpose of characterizing the granites used and their state of decay. We performed mineralogical observations and chemical analyses for this purpose. For understanding the decay factors that affect such granite, we considered several variables, such as the type of granite and the influence of environmental factors.

The only study known for this area provided evidence of several processes of decay due to the effect of seaside spray in buildings close to the coastline and other decay processes in areas far from the coastline, due to the humid environmental conditions that enhance biological colonization [26]. However, more studies are needed to help explain the main processes that may be responsible for the decay of granite buildings in the area, as some factors, such as environmental pollution, type of granite, and large timescale exposure to some atmospheric conditions, including the development of surface coatings, have not been previously considered. For this purpose, both mineralogical and geochemical studies

on the stone surfaces of buildings are performed in this work to assess the weathering of the granite blocks caused by the mentioned environmental factor.
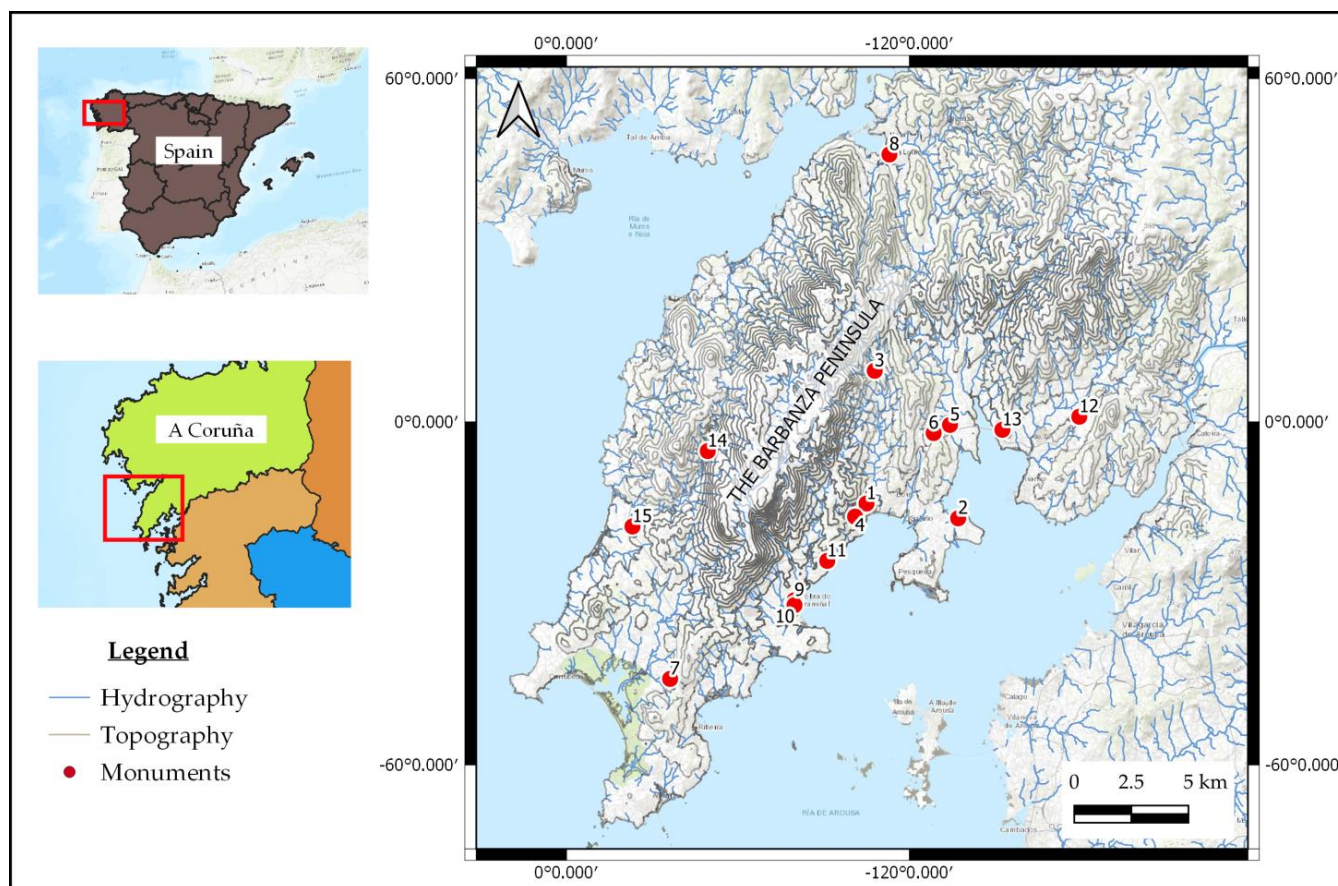

Figure 1. Location of samples on the topographic map of the Barbanza Peninsula (Galicia, Spain).

2. Materials and Methods

2.1. Study Area

2.1.1. Geography

The Barbanza Peninsula is the northernmost peninsula located on the western coast of Galicia. It is located between the estuaries of Arousa (to the South) and Muros-Noia (to the North) (Figure 1). At 416 km^2, it is limited by the Sierra de Barbanza, a mountain chain of more than 6 km long that runs longitudinally to the peninsula, in a NE-SW direction, with an average altitude that is 500 m above sea level. The top of the mountains is formed by small plateaus, with a top height of 687 m. We can divide the peninsula into two large areas: slopes (with pronounced and abrupt escarpments) and the coastal platforms, with an altitude less than 200 m located to the north and southeast, alternating beaches, sandbanks and rocky cliffs.

2.1.2. Climatological Setting

The Barbanza Peninsula belongs to the Humid Ocean domain [27], with a reduced annual thermal oscillation and high rainfall, with the maximum rainfall in winter months (about 40% of the annual total) [28] and a pronounced tendency towards summer aridity.

The range of annual precipitation is very wide, from below 900 mm in the coastal area to more than 3300 mm at the top of the mountains. A significant correlation is observed between precipitation and altitude with a W-E gradient. Thus, in Ribeira, with an average altitude of 5 mbsl, (W of the peninsula), the annual precipitation is around 1250 mm, while Boiro, in the eastern part (average altitude 32 mbsl), is about 2000 mm.

The average temperature ranges between 18.5 °C in summer and 9.5 °C in winter, with a significant gradient with altitude, especially noticeable in the duration of the seasons. The contrasts between the shore area (coastal platform) and elevated areas of the peninsula (the slopes) are significant, for instance, in frost days, not reported in the shore area but frequent in winter at the top areas.

Prevailing winds come from the SW in winter, with common storms, and from N to NE in summer. The highest speeds are usually reached during spring, ranging from 20 to 40 km/h, although sometimes (in autumn) reaching 80 km/h.

2.1.3. Geology

The Peninsula Barbanza includes several stone types, with a clear predominance of granite [29]. Among the types of granites, the one with the greatest representation is the granite with two micas of medium-coarse grain, called the Barbanza type, the majority in the entire central sector. In the Corrubedo area (SW), a fine-grained variant is present. Examples of churches with Barbanza-type granite are the churches of San Xoán de Macenda and San Pedro de Ribasieira (Figure 2).

Table 1. Characteristics of monuments studied.

|	Name of the Architecture	Location	Lithology	Distance to the Sea (km)	Altitude (m)	Categories of Populated Places	Construction Age (Century)	Sample
1	Pazo de Goians	Boiro	Granite and Metamorphic Rocks	0.5	20	Hamlet	XVII-XVIII	BO9AP
2	Church of San Cristobal de Abanqueiro	Boiro	Granite (two types)	0	6	Hamlet	XIII	BO4
3	Church of San Andres de Cures	Boiro	Granite (two types)	7	156	Hamlet	Romanic	BO1A BO1B
4	Church of Santiago de Lampón	Boiro	Granite	0.4	32	Hamlet	XII	BO7
5	Church of San Vicenzo de Cespón	Boiro	Granite	1.2	45	Hamlet	XII	BO8
6	Chapel Nosa Señora de Loreto	Boiro	Granite and Metamorphic Rocks	1.3	85	Hamlet	?	BO5
7	Church of San Xian de Artes	Ribeira	Granite	2	10	Hamlet	XVIII	RIB1
8	Church San Martiño de Noia	Noia	Granite (two types)	0.1	9	Village	XV	NO5
9	Pazo de Couto	Puebla del Caramiñal	Granite and Metamorphic Rocks	0.3	25	Village	XVIII	PU2P
10	Church of Santiago da Pobra do Daen	Puebla del Caramiñal	Granite and Metamorphic Rocks	0.2	20	Village	XVI	PU4A PU4B
11	Pazo da Merce	Puebla del Caramiñal	Granite and Metamorphic Rocks	0	18	Hamlet	XV	PU3AP
12	Pazo dos Torrado de Asadelos	Rianxo	Granite	3	60	Hamlet	XVI	RIA4P
13	Church of Divino Salvador de Taragoña	Rianxo	Granite	0.5	36	Hamlet	?	RIA06
14	Church of San Pedro de Ribasieira	Porto Son	Granite	4.5	167	None	XVIII	PO3
15	Church of Santa Mariña de Xuño	Porto Son	Granite	1.3	29	Hamlet	XII	PO4
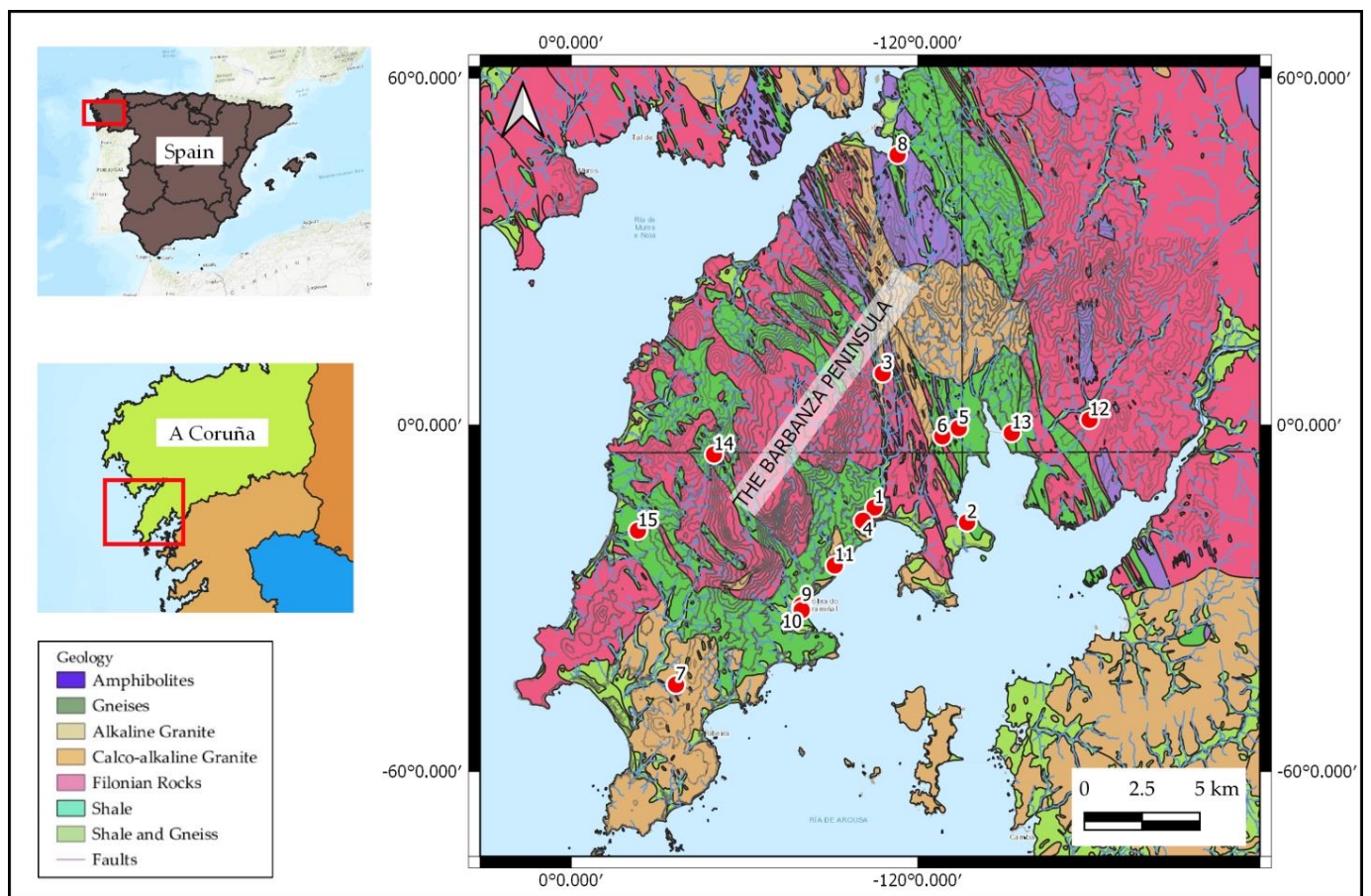
Figure 2. Geology of the Barbanza Peninsula (Galicia, Spain). The red circles with numbers provide the location of the studied churches, specified in Table 1.

Another type of granite form is part of the Migmatitic Domain: oriented, glandular granitic rocks that have undergone a process of migmitization and later metasomatism are distinguished. This type of oriented granite is visible in churches such as San Martiño de Noia (Figure 2). In the NE of the peninsula, the Noya Complex is found, which is formed of granite of two medium-grain micas.

Other rock types present are shale, gneiss and other metamorphic materials that make up the blastomylonitic pit. Some of the studied buildings include these rock types, although scarce, which are not included in this study.

2.2. Description of Buildings and Studied Variables

This study is carried out in a total of 15 architectural monuments distributed throughout the Barbanza peninsula (Figure 1) and covering the community of Boiro, Rianxo, Noia, Ribeira, Porto do Son and Puebla del Caramiñal. The types of monuments are churches, chapels with significant value and country houses. The following table (Table 1) summarizes some of the characteristics of each of these monuments, considering the factors to take into account that may contribute in different ways to the degree of deterioration, that is, location (with possible effect of air pollution in the largest villages), lithology (type of granite), altitude (significantly correlated with rainfall), distance to the sea (significantly correlated with seaside effect) and construction period (to check if there is any age vs. decay correlation). Our initial hypothesis is that the decay of the granite in the buildings, including chemical weathering of coating development, is correlated with one or some of the referred variables.

2.3. Sampling Procedure and Experimental Process

A total of 15 monuments were studied during the summer season of 2021, as indicated in Table 1. Given that sampling is a very restricted action in cultural heritage studies, in order to limit the impact on the stone material to be studied, small quantities of samples were collected in the surroundings of the monuments (material previously detached from walls and columns). A total of 17 granite samples were collected, as indicated in Table 1. For instrumental analyses, a portion of the dried samples was separated and homogenized to be analyzed using X-ray fluorescence spectroscopy.

2.3.1. X-ray Fluorescence (XRF)

Bulk samples were crushed into a powder with grain size below 63 μm. Three aliquots of each sample were prepared and measured. The elemental analyses of the samples were performed using a Fluorescence Spectrometer S4 Pioneer with a wavelength dispersion of Bruker–Nonius under helium purge.

2.3.2. Scanning Electron Microscopy (SEM) Coupled with Energy-Dispersive X-ray Spectrometry (EDS)

Some of the samples taken that exhibited stone coatings were studied and analyzed under scanning electron microscopy. Observations and analyses were performed on polished cross-sections previously covered by gold coating to obtain information about micromorphology and chemical composition (in terms of major elements) of the stone surface. Analyses were performed with an SEM (Cambridge Instruments, version 360 Stereoscan, Cambridge, UK), equipped with a microanalyzer in energy-dispersive spectrometry (EDS) (EDAX model) with an ultrathin (UHT) window in order to ensure the detection of light elements. The operating conditions were set at an accelerating voltage of 20 kV, beam current of 0.2 mA, acquisition time of 100 s and dead time of 30%–35%.

Elemental analyses were carried out according to standard mode and normalized by weight (%). The detection limit for the EDS system is approximately 0.1% weight. The accuracy of the analysis was periodically tested on standard USGS samples. Chemical analyses of the crust surfaces were performed in raster mode.

2.3.3. Petrographic Microscopy (PM)

Representative thin rock sections were prepared for petrographic study. The thin sections (30 μm) were observed under a polarizing microscope (Leica DM4500 P, University of A Coruña), equipped with a digital FireWire Camera Leica DFC 290 HD that worked with the Leica application suite software LAS 4.

3. Results and Discussion

3.1. Macroscopic Characterization of Coating on Stone Surfaces

The studied buildings showed different patterns of deterioration [11], as well as different possible coatings and chromatic alterations probably correlated with chemical weathering processes (Figure 3). Table 2 summarizes the occurrence of these features, including coatings. They were subdivided according to composition and thickness characteristics. Thus, the terms "film", "patina" and "crust" are used according to the thickness of the coating (respectively, from lowest to highest thickness) [11].

All the studied monuments show biological growth, mostly biofilms, especially associated with colonization of lichens (Figure 3a–c). Another predominant feature is the discoloration related to moisture stains (Figure 3d), which sequentially favors the formation of biofilms. Discoloration is also frequently observed, related to oxide stains (or staining) (Figure 3e,f) or bleaching patches due to the leaching of runoff water (Figure 3g). To a lesser extent, Fe-rich patinas, carbonate coatings, black crust (Figure 3g) and salt crusts have been observed (Figure 3h).
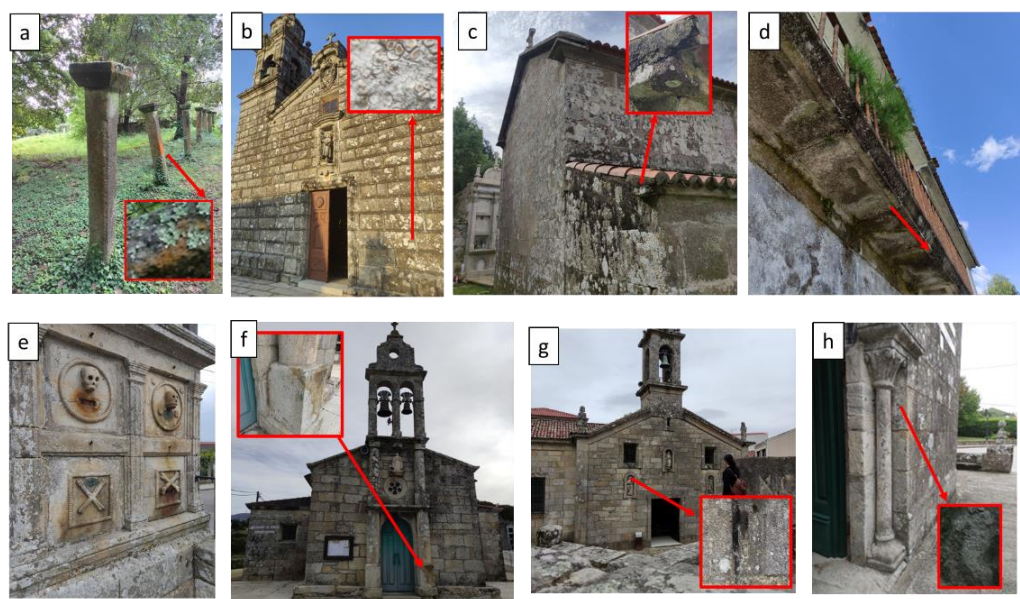
Figure 3. Macroscopic evidence of coating on stone surfaces. Boxes refer to the sample collection site for microscopic analysis: (**a**) Colonization of lichens in Pazo de Goians; (**b**) colonization of white lichens in Church of Santiago de Lampón; (**c**) biofilm in Church of Santa Maria de Ribasieira; (**d**) moisture stains in Pazo da Merce; (**e**) Church of San Vicenzo de Cespón; (**f**) discoloration related to oxide stains in Church of Santa Mariña de Xuño; (**g**) discoloration in Church of Santiago da Pobra do Daen; (**h**) salt crusts in Church of San Cristobal de Abanqueiro.

Table 2. Coatings and discoloration occurrences in the studied monuments.

	Coating					
	Fe-Rich Patina	Carbonate Coating	Black Crust	Salt Crust	Biofilm	Discoloration
Pazo de Goians					+++	
Church of San Cristobal de Abanqueiro		+		++	+	++
Church of San Andres de Cures					+++	+
Church of Santiago de Lampón		+			+	+
Church of San Vicenzo de Cespón	+				++	++
Chapel Nosa Señora de Loreto	+			+		++
Church of San Xian de Artes					+	+
Church San Martiño de Noia				+	+	++
Pazo de Couto					++	
Church of Santiago da Pobra do Daen		+	+		+	+
Pazo da Merce		+			+++	+
Pazo dos Torrados					+++	
Church of Divino Salvador de Taragoña					+	+
Church of Santa Maria de Ribasieira					+++	
Church of Santa Mariña de Xuño					++	+

3.2. Geochemical Analysis of the Stone Materials

The concentrations of the major and minor oxides of the monument samples are presented in Table 3. According to the classification of plutonic rocks of Middlemost [30],

most of the rocks are granites and quartz monzonites. Only the PU2P sample falls in the Syenite area.

For the geochemical analysis, bulk elemental composition and descriptive statistics for the studied samples are provided in Tables 3 and 4. Some correlations between elements as oxides are also shown in Figure 4.
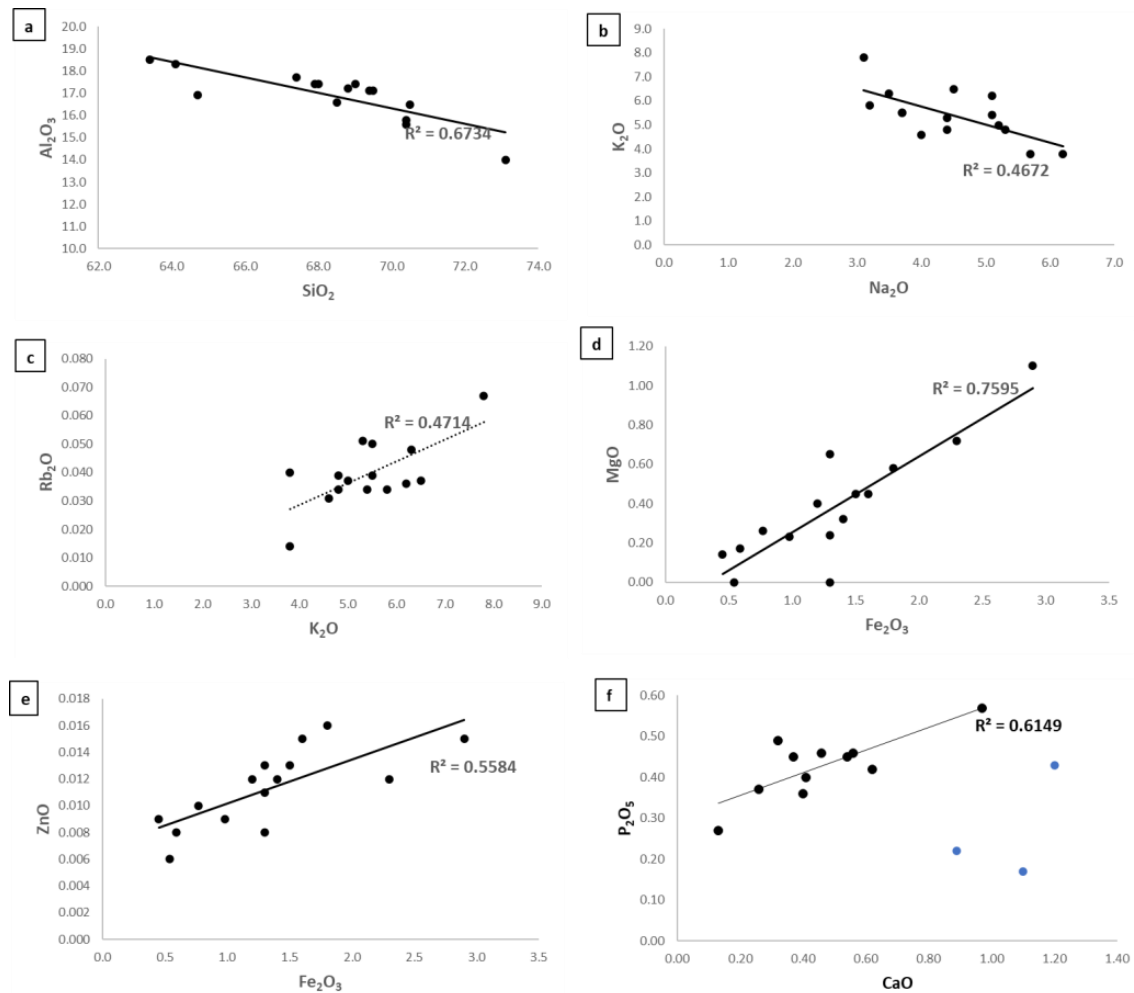

Figure 4. Geochemical correlation diagrams of major and minor elements. (**a**) Al_2O_3 vs. SiO_2 (**b**) K_2O vs. Na_2O (**c**) Rb_2O vs. K_2O (**d**) MgO vs. Fe_2O_3 (**e**) ZnO vs. Fe_2O_3 (**f**) P_2O_5 vs. CaO.

The samples presented an average concentration of SiO_2 of 68.3% and Al_2O_3 in the order of 16.9%. Both show an inverse trend among them (Figure 4a), as expected, due to their contents in feldspars and micas. The average content of Na_2O is in the order of 6.2%, due to the content in plagioclase. Na_2O shows an inverse correlation with K_2O (Figure 4b), with a content in the order of 7.8%. Potassium is found mainly in micas and potassium feldspars, so, as expected, granites with higher potassium feldspars will contain less plagioclase. There is also a positive trend between K_2O and Rb_2O (Figure 4c). Potassium and rubidium have similar charges, and substitutions may exist between them. Fe_2O_3 has an average concentration of 2.9%, which may be associated with biotite and Fe-oxides, while oxides, such as MgO, MnO and CaO, have concentrations of less than 1.5%. There is a significant positive correlation between oxides of Fe_2O_3 and MgO (Figure 4d), fundamentally due to the content in biotite and with ZnO related mainly to Fe-Zn oxides (Figure 4e). These elements are interesting as the oxidation of Fe and Mn due to chemical and biological processes usually results in visible chemical weathering effects such as stains and coatings [14,25].

Table 3. Chemical composition of the samples in % by XRF.

	SiO_2	Al_2O_3	K_2O	Na_2O	Fe_2O_3	CaO	MgO	P_2O_5	TiO_2	Rb_2O	ZnO	ZrO_2	SrO	CuO	SO_3	MnO	Y_2O_3	BaO	As_2O_3	LOI
PU4A	73.1	14.0	5.0	5.2	1.3	0.51	0.00	0.00	0.073	0.037	0.013	0.015	0.00	0.005	0.00	0.021	<0.003	<0.008	<0.010	0.6
PU4B	63.4	16.7	5.0	5.9	1.9	1.5	1.1	0.48	0.42	0.024	0.007	0.029	0.028	0.010	0.058	0.00	<0.003	0.093	1.1	2.2
Ria06	70.4	15.6	4.8	5.3	0.98	0.62	0.23	0.42	0.10	0.034	0.009	0.006	0.007	0.00	0.00	0.015	<0.003	<0.008	<0.010	1.4
BO9AP	67.9	17.4	6.2	5.1	0.77	0.41	0.26	0.40	0.11	0.036	0.010	0.007	0.008	0.008	0.00	0.00	<0.003	<0.008	<0.010	1.3
NO5	64.7	16.9	6.3	3.5	1.8	1.2	0.58	0.43	0.36	0.048	0.016	0.029	0.010	0.006	1.2	0.014	<0.003	<0.008	<0.010	2.7
PU2P	64.1	18.3	6.5	4.5	2.3	0.89	0.72	0.22	0.36	0.037	0.012	0.025	0.020	0.005	0.00	0.029	<0.003	0.11	<0.010	1.6
BO7	70.4	15.8	5.3	4.4	1.2	0.54	0.40	0.45	0.18	0.051	0.012	0.007	0.006	0.006	0.00	0.015	<0.003	<0.008	<0.010	1.2
BO8	69.4	17.1	7.8	3.1	0.54	0.13	0.00	0.27	0.026	0.067	0.006	0.00	0.004	0.005	0.00	0.066	<0.003	<0.008	<0.010	1.3
Ria04	68.5	16.6	3.8	5.7	1.3	1.1	0.65	0.17	0.20	0.014	0.008	0.013	0.031	0.00	0.00	0.020	<0.003	0.058	<0.010	1.6
Rib01	69.0	17.4	5.4	5.1	0.59	0.46	0.17	0.46	0.060	0.034	0.008	0.005	0.007	0.00	0.0	0.011	<0.003	<0.008	<0.010	1.2
BO5	70.5	16.5	3.8	6.2	0.5	0.32	0.14	0.49	0.041	0.040	0.009	0.004	0.00	0.007	0.00	0.011	<0.003	<0.008	<0.010	1.5
PO4	69.5	17.1	4.8	4.4	1.3	0.26	0.24	0.37	0.11	0.039	0.011	0.006	0.005	0.005	0.00	0.018	<0.003	<0.008	<0.010	1.7
PO3	68.0	17.4	5.5	3.7	1.6	0.40	0.45	0.36	0.24	0.039	0.015	0.014	0.008	0.005	0.00	0.011	<0.003	<0.008	<0.010	2.2
PU3AP	67.4	17.7	5.5	3.7	1.5	0.56	0.45	0.46	0.20	0.050	0.013	0.012	0.006	0.005	0.00	0.025	<0.003	<0.008	<0.010	2.4
BO4	68.8	17.2	5.8	3.2	1.4	0.37	0.32	0.45	0.20	0.034	0.012	0.012	0.007	0.005	0.00	0.00	<0.003	<0.008	<0.010	2.1
BO1B	63.4	18.5	4.6	4.0	2.9	0.97	1.1	0.57	0.46	0.031	0.015	0.033	0.017	0.00	0.00	0.037	<0.003	0.064	<0.010	3.3
BO1A	75.9	14.4	4.9	0.76	0.99	0.086	0.63	0.13	0.06	0.026	0.014	0.00	0.008	0.007	0.00	0.00	<0.003	<0.008	<0.010	1.9

Table 4. Descriptive statistics of the parameters and chemical elements of the samples studied.

	SiO$_2$	Al$_2$O$_3$	K$_2$O	Na$_2$O	Fe$_2$O$_3$	CaO	MgO	P$_2$O$_5$	TiO$_2$	Rb$_2$O	ZnO	ZrO$_2$	SrO	CuO	SO$_3$	MnO	Y$_2$O$_3$	BaO	As$_2$O$_3$	LOI
Total samples	63.4	14	3.8	3.1	0.45	0.13	0	0	0.026	0.014	0.006	0	0	0	0	0	0	0	0	0.6
Minimum	73.1	18.5	7.8	6.2	2.9	1.2	1.1	0.6	0.5	0.1	0.0	0.0	0.0	0.0	1.2	0.1	0.0	0.1	0.0	3.3
Maximum	68.3	16.9	5.4	4.5	1.3	0.6	0.4	0.4	0.2	0.0	0.0	0.0	0.0	0.0	0.1	0.0	0.0	0.0	0.0	1.7
Average	2.616	1.122	1.044	0.940	0.662	0.317	0.294	0.146	0.129	0.012	0.003	0.010	0.008	0.003	0.310	0.016	0.000	0.034	0.000	0.687
Standard deviation	3.83	6.64	19.30	21.01	49.82	54.34	77.16	39.77	71.15	29.64	25.87	76.52	88.67	65.86	387.30	82.57	-	218.38	-	39.51
Coef of var. (%)	63.4	14	3.8	3.1	0.45	0.13	0	0	0.026	0.014	0.006	0	0	0	0	0	0	0	0	0.6

Other elements, such as P_2O_5, are present in all samples with an average of 0.4% and showing a positive correlation with CaO (Figure 4f), probably due to the formation of apatite, carbonatoapatite and hydroxyapatite [31] in granites. However, samples PU4A, NO5, PU2P and Ria04 did not show the same trend and may be related to stains or coatings caused by an external origin or, alternatively, low concentrations in K- and alkali feldspars, and some accessory minerals of granite rocks (Figure 4f). The samples with the highest concentration of calcium (Ria3, Ria4, Rib3, PU2P) also presented concentrations of barium oxide, related to substitutions between the Ca and Ba cations. Zr, Sr and Ba are trace elements whose contents tend to increase as the alteration of the granites in the monuments progresses, because they are poorly leached when compared with other more mobile elements, such as Ca, Na, K or Mn [23,32]. In addition, we cannot discard an external origin of one part of the CaO, at least in some monuments, as it has been demonstrated that such an element can come from dissolution of the lime of joint mortars in granite buildings [23]. Furthermore, only sample NO 5 recorded SO_3 (1.2%). It is likely that the content in the other samples is very low and cannot be detected by this technique.

Several relative chemical weathering indices have been used for the quantification of sample weathering (Tables 5 and 6), in an attempt to assess the weathering in the studied buildings and their correlation with the variables reported above. The calculations required for the assessment of such indices can be seen in Table 5, and more details are provided elsewhere [23,32]. While absolute chemical weathering indices allow for the assessment of the degree of weathering, comparing the studied samples with a fresh (non-weathered) rock specimen, relative indices provide a quick assessment of chemical weathering by comparing rock samples affected by chemical weathering in different degrees [23]. Correlations were also established between weathering indices (Figure 5) to check their reliability to provide a picture of the decay of the granites. Weathering indices have been proposed for the quantification of weathering in the natural environment and weathering rates after exposure to artificial weathering tests [23,31–42]. They usually provide scattered data, depending on the type of weathering (chemical or not), the rock heterogeneity and the rate of weathering. They can be either absolute or relative. Relative indices also allow for determining the weathering degree of different samples from the same rock type by comparing the proportion of some mobile (e.g., CaO, Na_2O, K_2O) and immobile oxides (e.g., Al_2O_3, Fe_2O_3, Si_2O), and they are expressed as ratios [31–42]. Alternative indices consider the loss on ignition (LOI) or the water content, reflecting the increase in weathering caused by the hydration of clays, and they are considered as sensitive to weathering under humid conditions [20,42–48]. On the contrary, absolute indices are based on the assumption that the fresh rock composition is known, being less applicable in building stone [23,31–47]. In general, the use of weathering indices on building stones is scarce, but they show an active potential for studying chemical weathering in all types of stone materials [23,43–47]. In this study, we tested the use of some indices that provided reliable results in granites from historical buildings in NW Spain [23]. Such indices, their formulas, acronyms and authorship are provided in Table 5. After assessing the indices, we concluded that the indices CIA, MWPI, SA, W_P, SI-Ti Index, Kr, ACN, AKR Rc are the most suitable to evaluate the weathering of the studied samples. It is clear that the correlation between two indices can be due, in part, to the fact that they use one or some oxides. However, as different indices use different oxides, we consider that their correlation provides some indications of decay and not only due to differences in the composition of granites. Indeed, comparing the correlations observed between the different indices for the area of Barbanza, with another similar study carried out with two different granites used in historical buildings of A Coruña (NW Spain), they are completely different [23]. We consider this as evidence that the prevalence of weathering is the cause of the differences, more than differences in the granite composition, although we also compared these two variables below (indices vs. granite type).

Table 5. Summary of chemical weathering indices used in this study.

Chemical Weathering Index	Key	Formula
Chemical Index of Alteration	CIA	$[Al_2O_3/(Al_2O_3 + CaO + Na_2O + K_2O)] \times 100$
Weathering Potential Index	WPI	$[(K_2O + Na_2O + CaO + MgO\text{-}H_2O)/(SiO_2 + Al_2O_3 + Fe_2O_3 + TiO_2 + K_2O + Na_2O + CaO + MgO)] \times 100$
Modified Weathering Potential Index	MWPI	$[(K_2O + Na_2O + CaO + MgO)/(SiO_2 + Al_2O_3 + Fe_2O_3 + K_2O + Na_2O + CaO + MgO)] \times 100$
Product Index	PI	$100*[SiO_2/(SiO_2 + TiO_2 + Fe_2O_3 + Al_2O_3)] \times 100$
Silica-Alumina Ratio index (RuxtonRatio)	SA	SiO_2/Al_2O_3
Parker index	W_p	$[(2Na_2O/0.35) + (MgO/0.9) + (2K_2O/0.25) + (CaO/0.7)] \times 100$
Vogt Ratio	VR	$(Al_2O_3 + K_2O)/(MgO + CaO + Na_2O)$
Si-Ti Index	Si-Ti Index	$(SiO_2/Al_2O_3)/[(SiO_2/TiO_2) + (SiO_2/Al_2O_3) + (Al_2O_3 + TiO_2)]$
Silica-Sesquioxide Ratio	Kr	$SiO_2/(Al_2O_3 + Fe_2O_3)$
Alumina-Sodium to Calcium Oxide Ratio	ACN	$Al_2O_3/(Al_2O_3 + K_2O + Na_2O)$
Alumina to Potassium-Sodium Oxide Ratio	AKR	$Al_2O_3/(K_2O + Na_2O)$
Alkaline Ratio	ALK	$[K_2O/(K_2O + Na_2O)] \times 100$
Sesquoxide content	SOC	$Al_2O_3 + Fe_2O_3$
Residual Coefficient	Rc	$(Al_2O_3 + Fe_2O_3)/(K_2O + Na_2O + CaO + MgO)$

Table 6. Calculated values for the chemical weathering indices used in this study.

|	CIA	WPI	MWPI	PI	SA	W_P	VR	SI-Ti Index	Kr	ACN	AKR	ALK	SOC	Rc
PU4A	56.66	43.48	74.18	69.04	93.24	0.00	0.00	59.35	52.86	46.43	36.59	0.00	19.23	3.38
PU4B	57.39	35.92	60.33	38.46	48.02	55.25	50.37	87.68	34.29	5.74	43.28	29.17	6.21	0.00
Ria06	59.27	42.44	72.40	50.78	47.55	30.30	75.00	66.67	69.39	40.91	21.43	100.00	0.00	1.06
BO9AP	59.77	50.28	76.35	49.68	37.07	33.33	72.33	67.07	59.02	40.00	30.43	50.00	100.00	0.00
NO5	60.57	51.72	50.51	45.69	53.14	41.85	49.60	82.95	48.48	1.27	49.15	0.82	0.49	0.52
PU2P	60.62	46.36	56.89	53.86	47.67	54.88	34.27	83.92	46.84	21.05	31.65	80.00	3.47	1.67
BO7	60.68	46.90	66.77	51.72	37.47	38.39	65.41	72.29	67.11	48.00	20.59	50.00	28.57	1.23
BO8	60.79	68.18	76.73	77.59	27.84	0.00	74.38	25.24	85.90	60.00	0.00	44.44	7.04	4.83
Ria04	61.03	33.19	68.92	40.00	56.88	63.23	42.82	79.05	40.00	15.38	20.31	100.00	0.00	1.19
Rib01	61.35	47.96	77.16	46.09	40.93	24.36	82.29	55.05	72.34	40.00	21.74	100.00	0.00	0.91
BO5	61.52	35.88	83.11	47.32	32.32	20.59	85.22	45.56	66.67	69.23	18.18	0.00	38.89	0.73
PO4	64.38	44.69	69.51	68.06	28.60	32.83	70.48	66.67	63.93	50.00	17.65	50.00	21.74	1.05
PO3	64.44	48.89	61.06	59.48	32.03	42.25	55.13	79.47	53.42	40.54	36.84	61.54	31.25	0.50
PU3AP	64.46	49.33	59.49	55.35	36.84	40.07	63.71	74.35	62.50	41.94	25.00	54.55	16.67	1.03
BO4	64.73	54.10	59.04	61.14	31.52	32.59	64.66	79.05	53.97	38.71	50.00	58.33	100.00	0.00
BO1B	65.91	36.51	47.39	53.41	36.32	51.28	52.10	87.95	39.24	23.08	37.93	100.00	0.00	1.09
BO1A	71.48	67.31	38.66	56.06	9.86	75.54	60.19	55.56	55.32	63.64	0.00	53.33	100.00	0.00
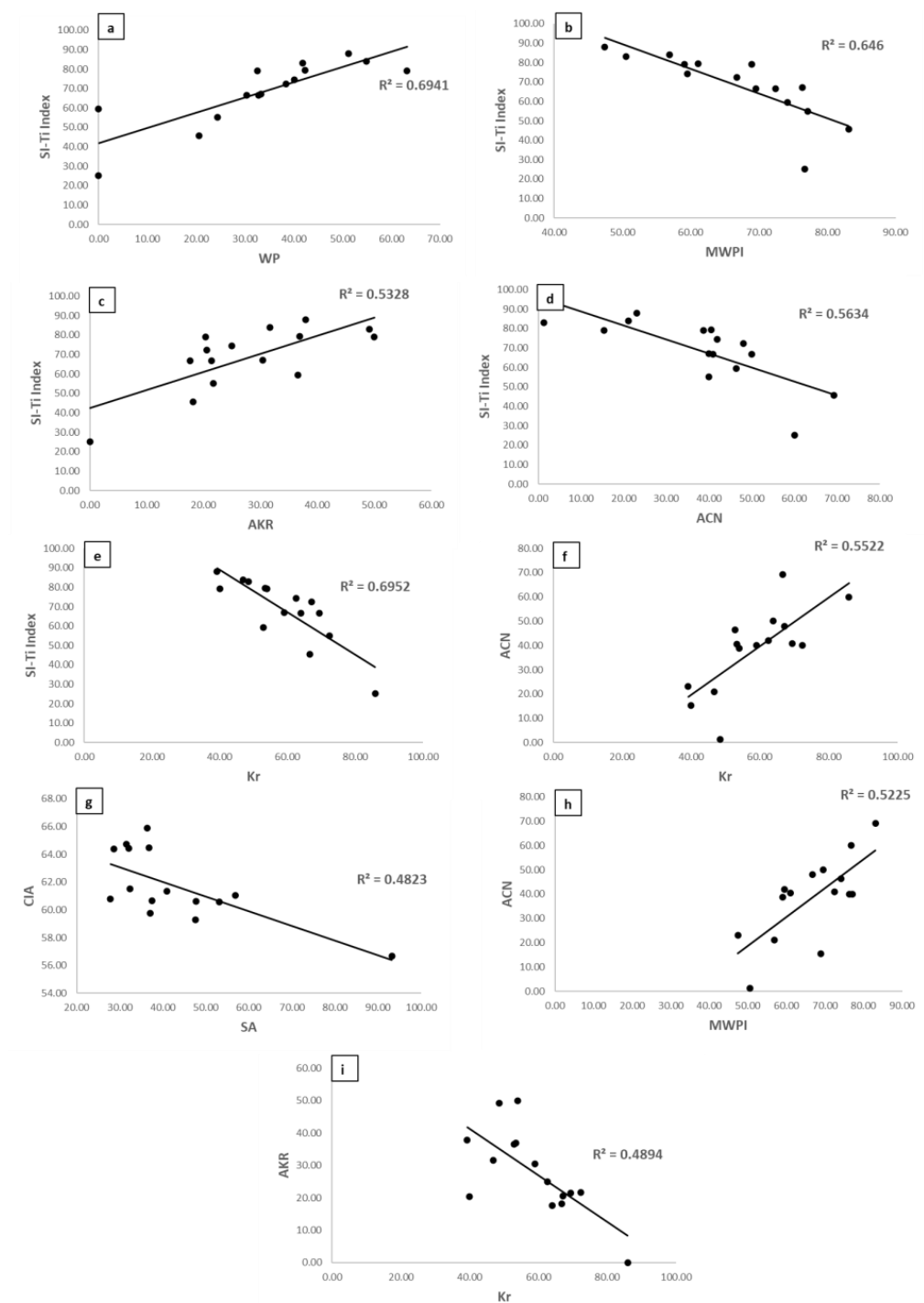
Figure 5. Geochemical correlation diagrams between some of the used weathering indices. (**a**) Si-Ti Index vs. WP (**b**) Si-Ti Index vs MWPI (**c**) Si-Ti Index vs. AKR (**d**) Si-Ti Index vs. ACN (**e**) Si-Ti Index vs. Kr (**f**) ACN vs. Kr (**g**) CIA vs. SA (**h**) ACN vs. MWPI (**i**) AKR vs. Kr.

The correlation of such indices vs. the studied variables was also observed. Taking the selected weathering indices, we compare them with the different considered variables. We consider that there is a linear correlation when the coefficient is above 0.5. Comparing the different weathering indices with the distance of the buildings to the shore, we do not observe any clear trend. The CIA index alone provides a positive correlation coefficient with the distance, higher for buildings located far from the shore. As there are several factors that can be correlated with this distance (e.g., effect of the sea-salt spray, precipitation), we divided the buildings into two different groups to refine the two variables. A group

of buildings called Area 1 corresponds to those located at less than 500 m from the shore, while buildings in Area 2 correspond to those located more than 500 m away. Looking at the indices of the two groups, some of them provide clear linear correlations between the distance and the indices (see Table 7). This is the case for the two groups for CIA, AKR and WPI for Area 1. In general, the lower the value of the index, the higher the weathering degree of the granite [23]. The indices that show a correlation with distance for Area 1 show a negative correlation, indicative of more weathering degree at higher distances inland from the shoreline. As in the Barbanza Peninsula, there is a correlation of rainfall and humidity with distance to the sea, which could be the main cause of more decay in buildings far from the sea shore, at least until a distance of 500 m.

Table 7. Linear correlation coefficients obtained for several weathering indices vs. distance to the sea: Area 1 (buildings located at 0–0.4 km), Area 2 (buildings located at >0.5 km). Bold numbers show significantly linear correlation (values below −0.5 or above 0.5).

Index	Area 1	Area 2	All
CIA	**−0.59**	**0.80**	**0.52**
WPI	**−0.67**	0.34	−0.39
MWPI	0.37	**−0.91**	−0.11
PI	−0.13	0.08	−0.10
SA	0.18	0.01	−0.20
W_P	0.46	**0.59**	0.36
VR	−0.31	**−0.71**	−0.02
Si-Ti Index	−0.14	**0.63**	0.26
Kr	0.16	**−0.72**	−0.40
ACN	0.14	**−0.55**	−0.18
AKR	**−0.56**	**0.62**	0.05
ALK	0.13	0.37	0.44

We do not observe the same result for Area 2 (distance above 500 m from the sea shore). Several more indices seem to fit better for Area 2, showing a clear correlation for MWPI, WP, VR, Si-Ti Index, Kr, ACM and ALK (Table 7 and Figure 6). However, half of them show a negative trend with distance while the other half show a positive trend. As most of them use the same elements, with different equations (see Table 5), we can consider that they provide evidence of a lower weathering degree in areas far from the sea. Looking at some of the plots (Figure 6), it can even be observed that there is a change in tendency from samples located at 1 km distance from the sea shore. So, it could be possible that the effect of sea salts can reach a higher distance (up to 1 km), with this area (between some hundreds of meters and 1 km distance to the sea) being where the effect of sea salt plus more humidity cause a more clear effect on granite, enhancing chemical weathering. Particularly, more samples should be considered to clarify this observation.

Considering other possible correlations, we checked the correlation coefficient between the altitude above the sea level and weathering indices. No significant correlations are observed for any samples. However, we divided the buildings again into two groups: Area 1 (<30 m above the sea level) and Area 2 (>30 m) (Table 8). For Area 1, a correlation was observed for indices WPI, MWPI and ACR. Both WPI and AKN showed a strong negative correlation. This is indicative of a higher weathering degree at more elevated altitudes. We consider that the other indices did not provide a clear correlation because of the small number of samples considered.
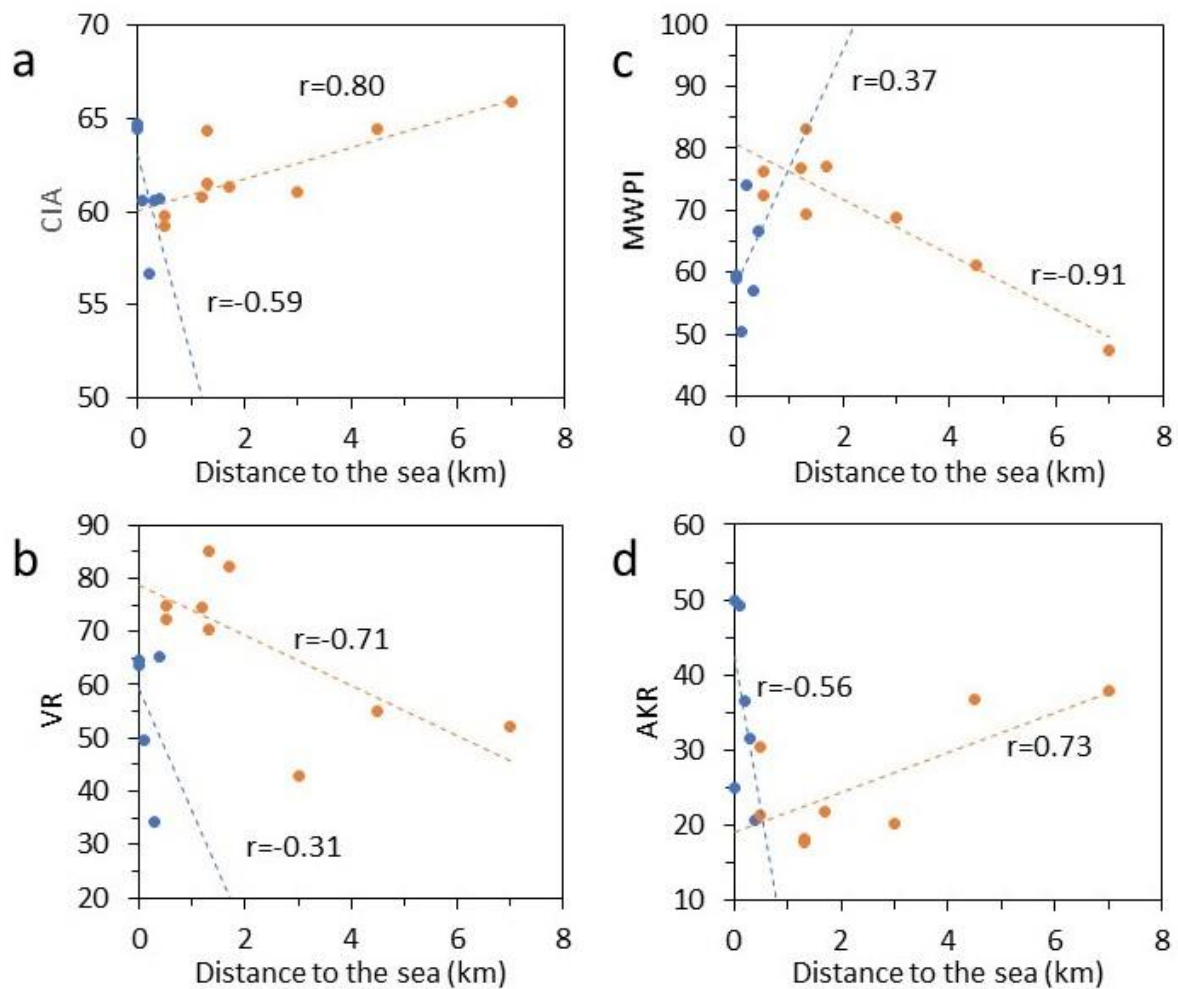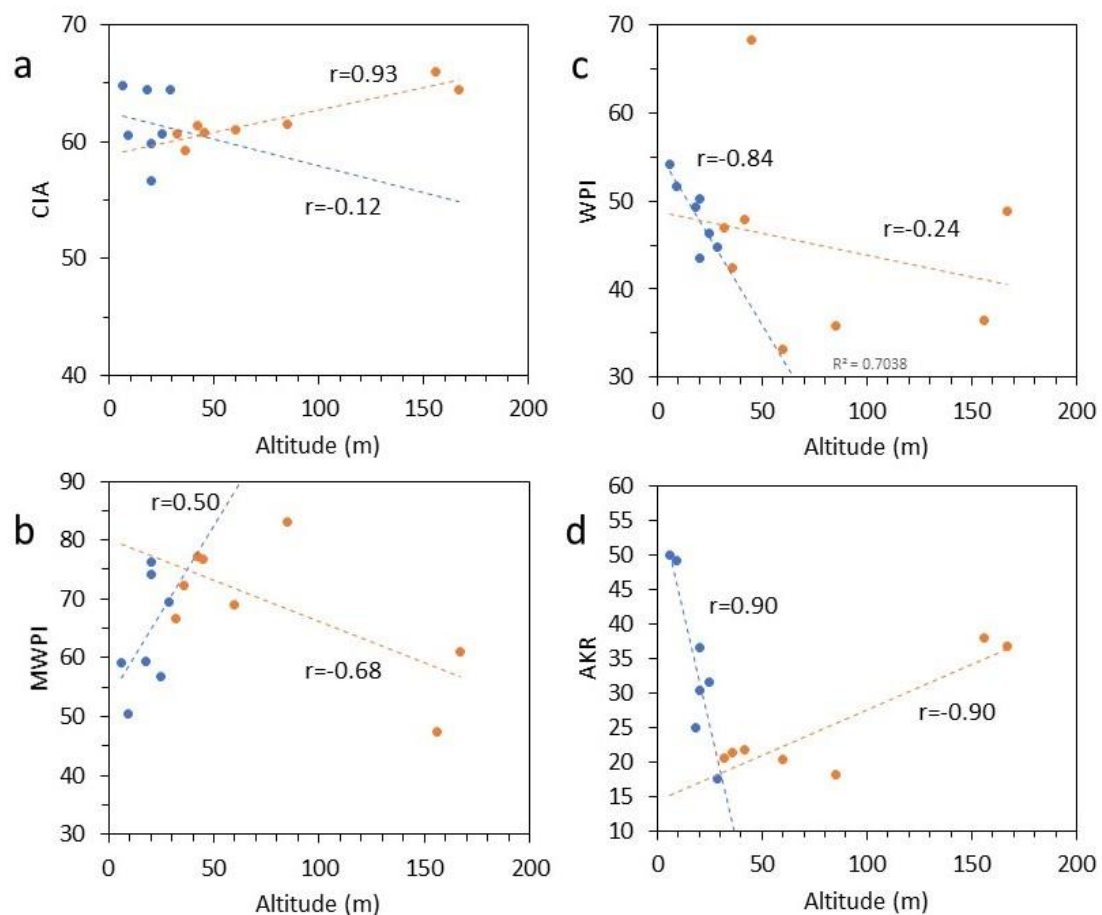
Figure 6. Geochemical correlation diagrams between some weathering indices and distance. The doted lines show probable correlations with the corresponding linear correlation coefficient of Area 1 (buildings located at 0–0.4 km, in blue) and Area 2 (buildings located at >0.5 km, in orange). (**a**) CIA vs. distance to the sea. (**b**) VR vs. distance to the sea. (**c**) MWPI vs. distance to the sea. (**d**) AKR vs. distance to the sea.

For Area 2, a significant correlation is observed for CIA, MWPI, Si-Ti Index, Kr and AKR (Figure 7). The MWPI shows a contrary trend to Area 1, while both CIA and AKR show a positive trend. In other words, there is a decrease in weathering with altitudes. Thus, it seems that there is a significant correlation between the weathering degree and altitude, which is different for the two areas. We can explain this because, as showed, buildings located close to the sea shore correspond to those located at lower altitudes, with one exception [26]. Thus, again, it is observed that the buildings located in a strip area some hundreds of meters from the sea shore and at lower altitudes (between 10 and 30 m) correspond to more weathered granites. In addition, in the Barbanza Peninsula, there is a significant correlation of altitude with total annual precipitation. Thus, precipitation (and humidity) is not the sole factor that enhances weathering; some precipitation (and humidity) ranges, summed to the sea-salt spray effect, may be involved in the increasing weathering rates of the granites. It is possible that in this strip of land, a mixture of sea spray and rainfall causes the dissolution of salts in rainfall, and this water is less acidic. As granite minerals, such as quartz, feldspars and micas, are resistant to dissolution and hydrolysis at acidic pH but not basic [49], the chemical weathering can be increased in this area. However, given the scarce number of samples used for this study, more research is needed to shed more light on this.

Table 8. Linear correlation coefficients of some weathering indices when compared with altitude above the sea level: Area 1 (buildings < 30 m) and Area 2 (buildings > 30 m). Bold values provide significant linear correlation (values below -0.5 and above 0.5).

Index	Area 1	Area 2	All
CIA	-0.12	**0.93**	0.47
WPI	**-0.84**	-0.24	0.34
MWPI	**0.50**	**-0.68**	0.19
PI	0.37	-0.09	0.06
SA	0.01	-0.33	0.26
W_P	0.22	0.31	0.21
VR	-0.02	-0.47	0.02
Si-Ti Index	-0.43	**0.50**	0.14
Kr	0.35	**-0.62**	0.26
ACN	0.42	-0.25	0.04
AKR	**-0.90**	**0.90**	0.01
ALK	0.31	-0.01	0.38

Figure 7. Geochemical correlation diagrams between some weathering indices and altitude. The doted lines show probable correlations with the corresponding linear correlation coefficient of Area 1 (buildings located <30 m above sea level, in blue) and Area 2 (buildings located >30 m above sea level, in orange). (**a**) CIA vs. altitude. (**b**) MWPI vs. altitude. (**c**) WPI vs. altitude. (**d**) AKR vs. altitude.

Looking at other possible variables, we considered the same ones related above (distance to the sea and altitude) with the type of granite, but we did not observe significant correlations. We also built three groups of samples considering the size of the population where the building is located. This is because historical buildings located in large populations can be exposed to higher air pollution concentrations. However, we did not observe any clear correlation with weathering indices, although it seems that it is possible that some indices can be different depending on this variable (Figure 8). Considering the biological colonization of surfaces, we built three groups of samples and compared weathering indices. As occurs with air pollution, there is no clear trend, although some indices could show some weak correlation.
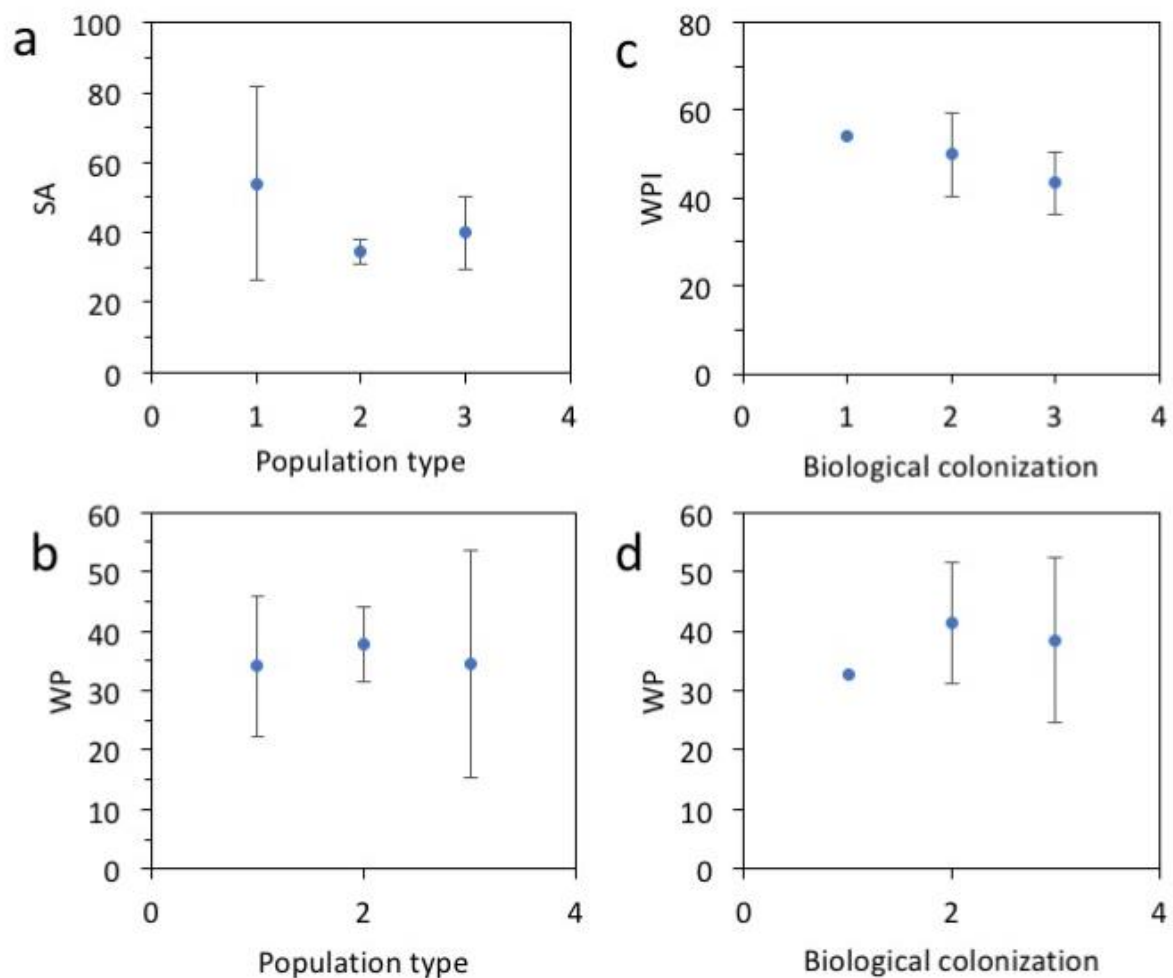
Figure 8. Geochemical correlation diagrams between weathering indices vs. other variables. The variables are presence of biological colonization and size of the population where the building is located. (**a**) SA vs. population type. (**b**) WP vs. population type. (**c**) WPI vs biological colonization category. (**d**) WP vs. biological colonization category.

Concluding, we did not observe any clear correlation between the staining of granite surfaces in buildings due to weathering because of the type of granite, biological colonization or deposition of air pollutants, while it seems that there may be a correlation with weathering that should be studied in more detail.

3.3. Microscopic SEM-EDS

The SEM-EDX of the samples from Pazo de Goians (B09AP), Pazo de la Merce (PU3AP) and Church of Ribasieira (PO3) is shown in Figures 9–11. From Figure 3, it is possible to see the location of the coating corresponding to each sample.
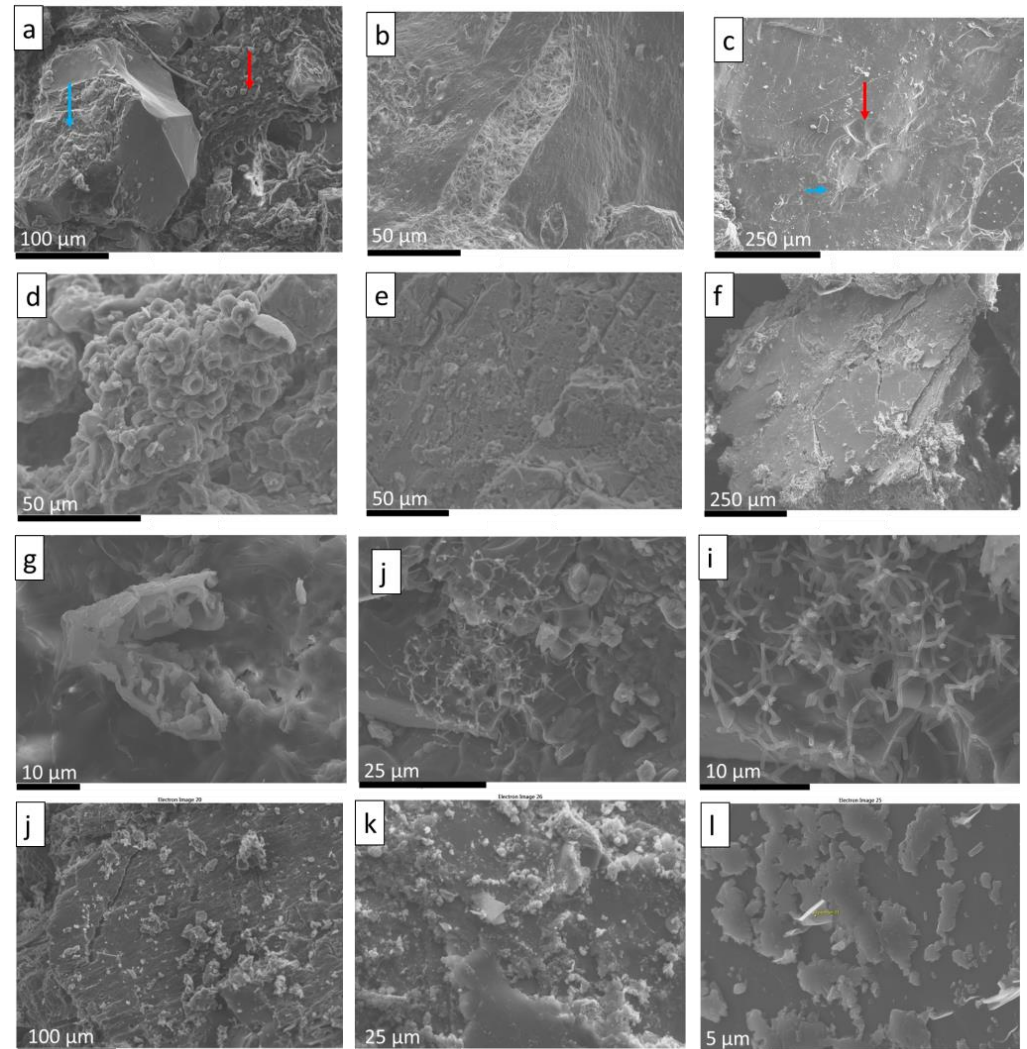
Figure 9. (**a**) Partially altered quartz (blue arrow) and salt coverage in sample BO9AP. (**b**) Partial dissolution of plagioclase, evidencing chemical weathering in the PU3AP sample. (**c**) Microtextures typical of quartz conchoidal fracture (blue arrow), and arcuate (red arrow) step (produced by fracturing processes) precipitation and solutions in PU3AP sample. (**d**) Biological colonization in the PU3AP sample. (**e**) Dissolution of crystal voids form plagioclase PU3AP. (**f**) Mica with fracturing and PU3AP precipitations. (**g–i**) Biological colonization PU3AP. (**j,k**) Precipitation of salts on the plagioclase surface in the PO3 sample. (**l**) Titanium Oxide crystal in PO3 sample.
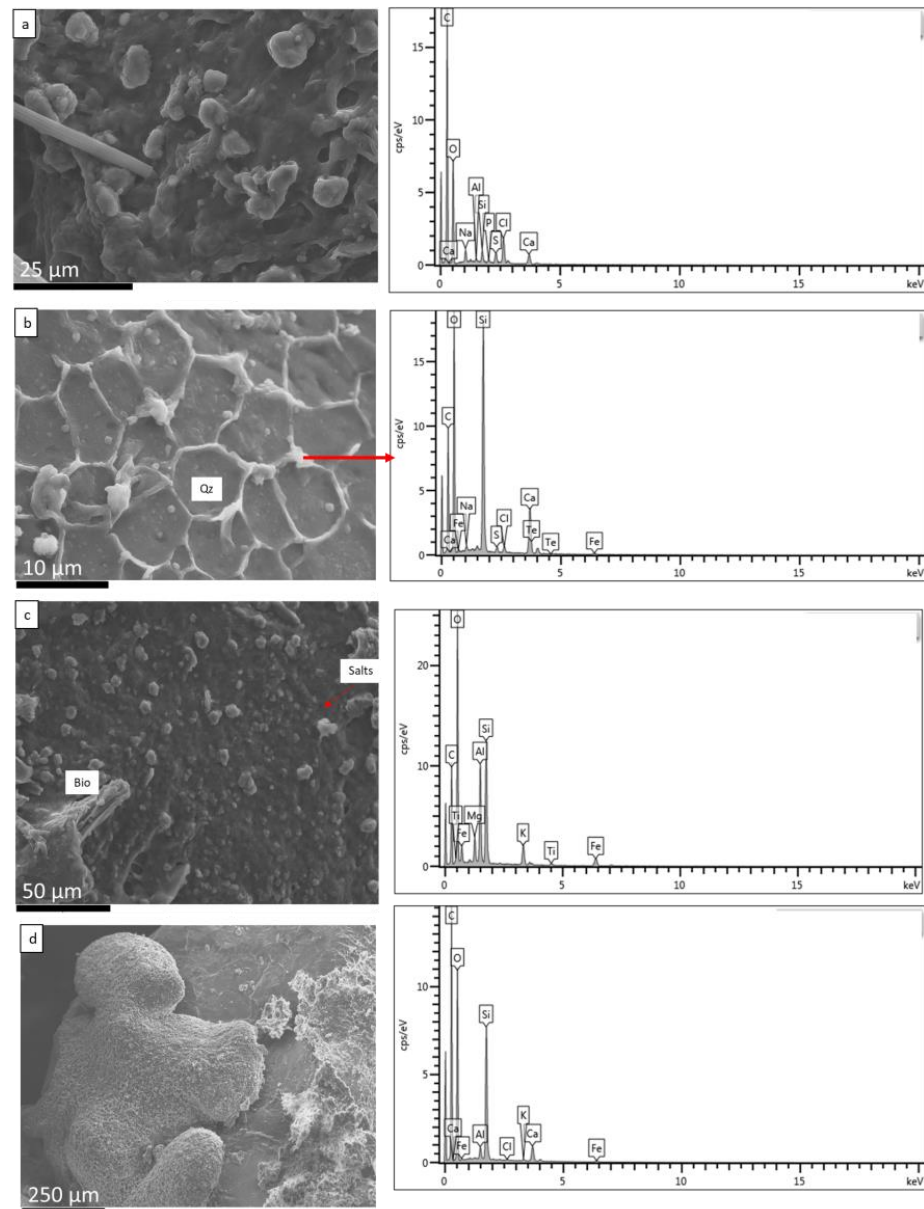
Figure 10. EDS analysis of the studied samples. (**a**) Evidence of the presence of Cl, S, P and C related to mineral neoformations in the BO9AP sample. (**b**) Formation of salts on quartz edges showing honeycomb microtexture; shows BO9AP. (**c**) Biotite crystal on the left and salt precipitation in the BO9AP sample. (**d**) Precipitation of calcium carbonate on the left in a K-feldspar crystal and salt crust on the right (Cl) in a PU3AP sample.

The most abundant minerals are identified from the micrographs as quartz, micas, K-feldspars and plagioclase. These minerals present surface alterations that show the chemical weathering of the rocks (Figure 9a,f). Plagioclase frequently presents altered surfaces, either via the dissolution or precipitation of minerals (Figure 9b,e). For its part, quartz shows characteristic microtextures, such as conchoidal fracture, straight and arcuate step (produced by fracturing processes), precipitation and dissolutions (Figure 9c). Through this technique, the presence of microorganisms in the studied samples is also evident. (Figure 9d,g,h,i)
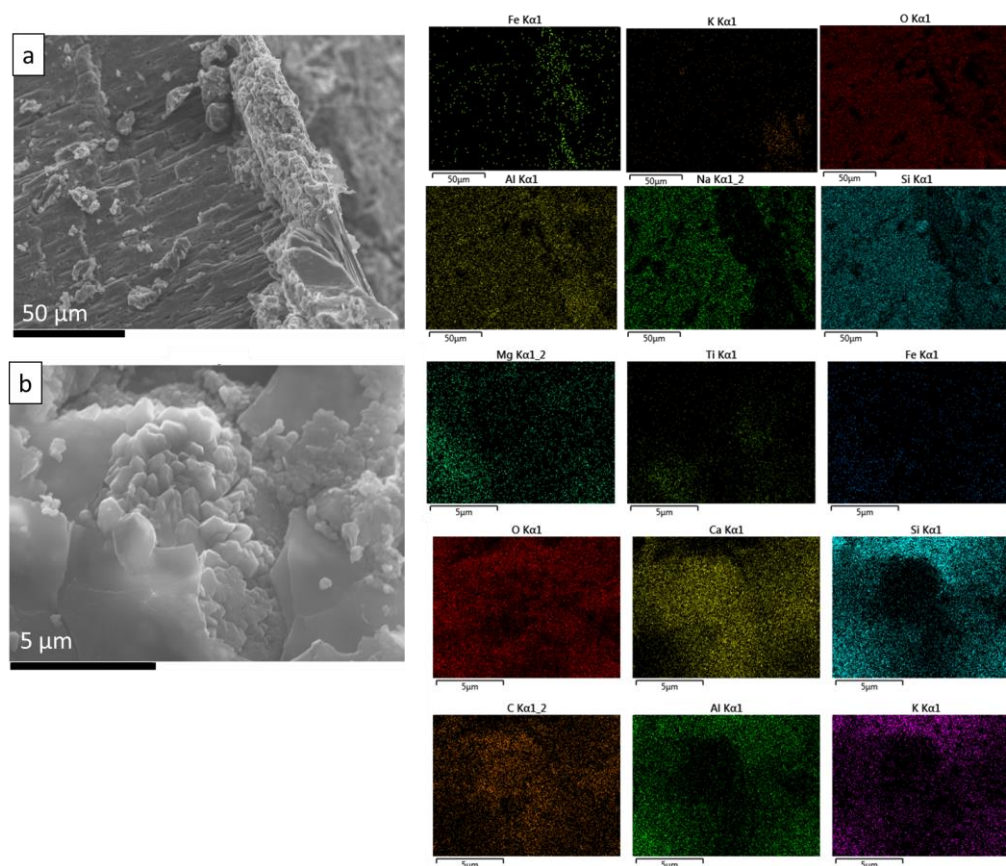
Figure 11. SEM-EDS maps of the PO3 sample. (**a**) Map showing the growth of iron alumnosilicate mineral at the edges of plagioclase. (**b**) Calcite crystal growth on feldspar.

The presence of Cl, S, P and C is related to the mineral neoformation, among which chloride salts (halite and calcium chloride), sulfates (possibly gypsum), amorphous calcium phosphates and carbonates (calcite, ankerite) stand out in samples BO9P and PU3AP (Figure 9j,k and Figure 10a–c). Both buildings are very close to the sea, thus evidencing the provenance and impact of the marine environment. Salt deposition, surface efflorescence and salt-rich coatings are expected in areas close to the sea [20–22,48,50]. Such salts will contribute to the deterioration of the monumental stone [1–3,20–22,48,50,51]. A recent work demonstrated that they decay granite in buildings in the Barbanza Peninsula [26]. The more spherical morphologies could be related to air pollution. In the BO9AP sample, the element Te was identified, possibly related to the same salts (Figure 9c). It is interesting and unexpected to find this element in this building, because it is located 500 m from the seaside. This is the area where the chemical weathering indices showed higher weathering.

Cl and S salts were not identified in the PO3 sample (Figure 11). On the contrary, the percentages of C, Si and P in abundance reveal the biological action, some identified by means of this technique, such as fungi and thallus lichens. This building is located in Area 2, 4.5 km from the sea shore at an altitude of 167 m. Despite this, the chemical weathering indices did not show significant weathering at this distance, but visible chemical weathering features of rock-forming minerals are also visible under the SEM. Thus, despite the weathering indices probably not being resolutive enough, the SEM provided evidence of weathering. Due to the presence of biological colonization and the high humidity and average annual precipitation, we cannot discard the biological weathering as responsible for these effects [14]. Indeed, Ti and Fe were identified under the SEM, previously reported in FRX, possibly related to oxides (Figure 9l).

3.4. Petrographic Analysis

Considering the discolorations in the superficial stone and the different lithologies in the study area, samples BO8, BO9AP, BO2, RIB1, PU3AP, PU2P and PU4A were selected for petrographic analysis. All of them are representative of the different variables considered (e.g., distance to the sea shore, altitude, lithology, etc.). The petrographic characteristics of the six selected samples are shown in Figure 12.
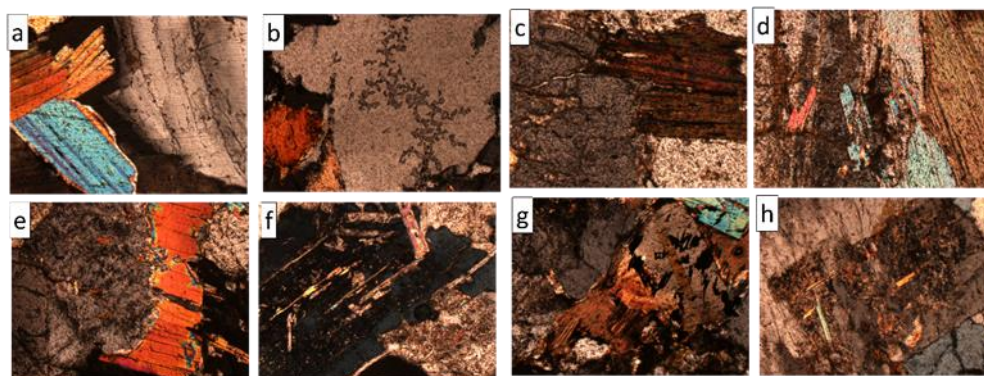

Figure 12. Photographs of the 7 selected samples (BO9AP, BO2, RIB1, BO8, PU3AP, PU2P, PU4A) from the study area. All samples are taken with crossed nicols, 4× magnification. Observe: Elongated muscovite crystals: (**a**) from sample RIB1. Plagioclase with sericitation; (**b**) from the BO8 sample. Plagioclase crystal, biotite; (**c**), muscovite and opaques; (**d**) in the BO9AP sample. Muscovite fracturing, plagioclase sericitation; (**e**) K-feldspar alteration; (**e**,**f**) and intra-granular cracks with muscovite crystals and plagioclase clays; (**f**) in sample B02. Opaque minerals (**g**) and plagioclase alteration (**h**) in PU2 sample.

The results are related to the mineralogical composition studied using XRD. Samples are granites, and the main minerals are quartz, plagioclase, feldspar and micas (mainly biotite and muscovite). The grain size is fine to medium grain in the BO8 (Figure 12b) and PU3 samples and medium to coarse grain in the rest, whose alteration is higher because the surface of minerals such as feldspars and micas is more exposed (Figure 12a,e).

Quartz occurs as polycrystalline aggregates with a non-uniform appearance. The plagioclases are mainly albite and oligoclase types with albite and pericline polysynthetic twinning (Figure 12a), sericitation (Figure 12b), oxides (Figure 12c,g) and, in some cases, mineralized cracks (Figure 12d). In some cases, plagioclase contains pores in the center of the crystal, where alterative minerals are formed, probably clays (Figure 12b,f). In some samples (Figure 12c,h), the feldspar appears highly weathered with fissures and intense reddish-brown pleochroism, indicating the presence of iron oxyhydroxides. On the other hand, the biotite of the BO9AP sample (Figure 12c) presents reflected iron leaching on the edges. This area corresponds to a building located 500 m from the sea shore and at an altitude of 20 m, with this area being the most affected by chemical weathering, as observed in weathering indices. Iron also presents small inclusions of accessory minerals (zircon and rutile). The BO8 sample (Figure 12a) shows a slight orientation of its grains marked by micaceous minerals. Thus, some weathering features can be observed in most buildings. This is indicative of two possible explanations: (i) there is a local component of the weathering and processes that cause the formation of stains and coatings, such as local architectural features or façade orientation [2,14,23,24]; (ii) there is some previous inherited weathering of the granites used in the construction of the buildings that must also be taken into account. To clarify these two possibilities, more samples should be studied in the future [8,14,23]

4. Conclusions

This study was carried out on granite rock surfaces of historical buildings in the Barbanza Peninsula (Galicia, NW Spain) to assess the degree of weathering in the built environment, the possible environmental variables that cause such weathering and to obtain more knowledge on the causes of decay and formation of coatings on the granite surfaces. Although the effect of some natural environmental factors, such as humidity, precipitation and the sea spray effect on stones, are well known, most of the existing knowledge comes from case studies on historical buildings. However, in this work, a group of historical buildings constructed with granite blocks was considered in an area with a steep climatic and sea spray gradient. A combination of geochemical, petrological and mineralogical studies has allowed us to obtain several unexpected conclusions.

1. Macroscopic studies provided the first evidence of several types of decay and the formation of coatings of buildings in the area, with physical decay more evident in some buildings located close to the sea shore, while both apparent chemical weathering and the development of coatings were more evident in buildings located far from the shoreline.
2. Chemical analyses, assisted by the use of weathering indices, showed, surprisingly, a higher chemical weathering degree in buildings located in a strip between a few hundreds and 500 m from the coastline. These buildings were also located at altitudes between 10 and 30 m above sea level. This area corresponds to more humid conditions than the shoreline and less humid than inland areas. Moreover, it is an area affected by sea spray to a lower degree than the shoreline area but a higher degree than inland areas. Thus, it is possible that sea spray combined with rainfall results in less acidity on the building surface water, which is more effective in the chemical weathering of granite minerals than acidic water. Still, more studies are needed to obtain more significant data.
3. After microscopic observations, we observed that salts were more present in buildings close to the sea shore, as expected, with these buildings being more affected by physical weathering. However, the development of stains and coatings could be correlated with other factors, such as architectural details or biological colonization. We found no evidence of a direct correlation with climate and sea spray.

References

1. Alves, C.; Figueiredo, C.A.; Sanjurjo-Sánchez, J.; Hernández, A.C. Effects of Water on Natural Stone in the Built Environment—A Review. *Geosciences* **2021**, *11*, 459. [CrossRef]
2. Amoroso, G.G.; Fassina, V. *Stone Decay and Conservation: Atmospheric Pollution, Cleaning, Consolidation and Protection*; Elsevier Science Publishers: Amsterdam, The Netherlands, 1984.
3. Sanjurjo-Sánchez, J.; Alves, C. Decay effects of pollutants on stony materials in the built environment. *Environ. Chem. Lett.* **2012**, *10*, 131–143. [CrossRef]
4. Tokmak, M.; Dal, M. Classification of Physical, Chemical and Biological Deteriorations Observed in Ankara Stone Monuments. *Int. J. Pure Appl. Sci.* **2020**, *6*, 8–16. [CrossRef]
5. Patil, M.S.; Kasthurba, A.K.; Patil, M.V. Characterization and assessment of stone deterioration on Heritage Buildings. *Case Stud. Constr. Mater.* **2021**, *15*, e00696. [CrossRef]
6. Özmen, A.; Sayın, E. Evaluation of material properties of cultural heritage building by destructive and non- destructive testing: Malatya Taşhoran Church case study. *Constr. Build. Mater.* **2023**, *392*, 131693. [CrossRef]
7. Steiger, M.; Charola, A.E.; Sterflinger, K. Weathering and deterioration. In *Stone in Architecture*; Siegesmund, S., Snethlage, R., Eds.; Springer: Berlin/Heidelberg, Germany, 2011.
8. Sanjurjo-Sánchez, J.; Vidal Romaní, J.R.; Alves, C. Comparative analysis of coatings on granitic substrates from urban and natural settings (NW Spain). *Geomorphology* **2012**, *138*, 231–242. [CrossRef]
9. Siegesmund, S.; Snethlage, R. *Stone in Architecture: Properties, Durability*; Springer: Berlin/Heidelberg, Germany, 2011.
10. Artesani, A.; Di Turo, F.; Zucchelli, M.; Traviglia, A. Recent advances in protective coatings for cultural heritage—An overview. *Coatings* **2020**, *10*, 217. [CrossRef]
11. ICOMOS-ISCS. Illustrated Glossary on Stone Deterioration Patterns. 2008. Available online: http://www.international.icomos.org/publications/monuments_and_sites/15/pdf/Monuments_and_Sites_15_ISCS_Glossary_Stone.pdf (accessed on 20 December 2023).
12. Elgohary, M. Air pollution and aspects of stone degradation "Umayyed Liwân—Amman Citadel as a Case Study". *J. Appl. Sci. Res.* **2008**, *4*, 669–682.
13. Tosunlar, K.M.M.; Beycan, A. Non-destructive test investigations on the deterioration of Roman Mausoleum in Karadag Central Anatolia, Turkey. *Mediterr. Archaeol. Archaeom.* **2020**, *20*, 199–219.
14. Sanjurjo-Sánchez, J.; Alves, C.; Freire-Lista, D.M. Biomineral deposits and coatings on stone monuments as biodeterioration fingerprints. *Sci. Total Environ.* **2023**, *912*, 168846. [CrossRef]
15. Biçen Çelik, A.; Ergin, Ş.; Dal, M.; Ay, İ. Analysis of Stone Deterioration on the Facades of Hatuniye Madrasah. *J. Archit. Sci. Appl.* **2023**, *8*, 355–369. [CrossRef]
16. Marrocchino, E.; Telloli, C.; Pedrini, M.; Vaccaro, C. Natural Stones Used in the Orsi-Marconi Palace Façade (Bologna): A Petro-Mineralogical Characterization. *Heritage* **2020**, *3*, 1109–1123. [CrossRef]
17. Freire-Lista, D.M.; Campos, B.B.; Moreira, P.; Ramil, A.; López, A.J. Building Granite Characterisation, Construction Phases, Mason's Marks and Glyptography of Nossa Senhora de Guadalupe Church, Mouçós e Lamares, Galicia-North Portugal Euroregion. *Geoheritage* **2023**, *15*, 24. [CrossRef]
18. Juhász, P.; Kopecskó, K. Evaluating effect of biomineralization compounds on the surface hardness and material loss of porous limestone. *Pollack Period.* **2013**, *8*, 175–186. [CrossRef]
19. Jo, Y.H.; Lee, C.H. Ultrasonic Properties of a Stone Architectural Heritage and Weathering Evaluations Based on Provenance Site. *Appl. Sci.* **2022**, *12*, 1498. [CrossRef]
20. Fitzner, B.; Heinrichs, K.; La Bouchardiere, D. Weathering damage on Pharaonic sandstone monuments in Luxor–Egypt. *Build. Environ.* **2003**, *38*, 1089–1103. [CrossRef]
21. Chabas, A.; Lefevre, R.A. Chemistry and microscopy of atmospheric particulates at Delos (Cyclades–Greece). *Atmos. Environ.* **2000**, *34*, 225–238. [CrossRef]
22. Goudie, A.S.; Viles, H.A. *Salt Weathering Hazards*; John Wiley & Sons: Chichester, UK, 1997.
23. Sanjurjo-Sánchez, J.; Alves, C.; Vidal-Romaní, J.R. Assessing the weathering of granitic stones on historical urban buildings by geochemical indices. *Earth Sci. Res. J.* **2016**, *20*, F1–F13. [CrossRef]
24. Sanjurjo-Sánchez, J.; Vidal-Romani, J.R.; Alves, C.A.S.; Fernández-Mosquera, D. Origin of gypsum-rich coatings on historic buildings. *Water Air Soil Pollut.* **2009**, *204*, 53–68. [CrossRef]
25. Sanjurjo-Sánchez, J.; Alves, C. Conservation of stony materials in the built environment. *Environ. Chem. Lett.* **2015**, *13*, 413–430.
26. Hernández, A.C.; Sanjurjo-Sánchez, J.; Alves, C.; Figueiredo, C.A.M. Comparative Study of Deterioration in Built Heritage in a Coastal Area: Barbanza Peninsula (Galicia, NW Spain). *Geosciences* **2023**, *13*, 375. [CrossRef]
27. Meteogalicia. 2023. Available online: https://www.meteogalicia.gal/ (accessed on 12 February 2023).
28. Sistema de Información de Ordenación del Territorio y Urbanismo de Galicia (SIOTUGA). 2023. Available online: http://siotuga.xunta.gal/siotuga/documentos/urbanismo/RIBEIRA/documents/0347ME016.pdf (accessed on 20 December 2023).
29. Parga-Pondal, D.I. Nota explicativa del mapa geológico de la parte NO de la provincia de La Coruña. *Leidse Geol. Meded.* **1956**, *21*, 467–484.
30. Middlemost, E.A. Naming materials in the magma/igneous rock system. *Earth-Sci. Rev.* **1994**, *37*, 215–224. [CrossRef]
31. Parker, A. An index of weathering for silicate rocks. *Geol. Mag.* **1970**, *107*, 501–504. [CrossRef]

32. Gupta, A.S.; Rao, K.S. Weathering indices and their applicability for crystalline rocks. *Bull. Eng. Geol. Environ.* **2001**, *60*, 201–221. [CrossRef]
33. Reiche, P. Graphic representation of chemical weathering. *J. Sediment. Petrol.* **1943**, *13*, 58–68.
34. Topal, T. Quantification of weathering depths in slightly weathered tuffs. *Environ. Geol.* **2002**, *42*, 632–641. [CrossRef]
35. Topal, T.; Sözmen, B. Deterioration mechanisms of tuffs in Midas monument. *Eng. Geol.* **2003**, *68*, 201–223. [CrossRef]
36. Vogel, D.E. Precambrian weathering in acid metavolcanic rocks from the superior province. Villebon Township. South-Central Québec. *Can. J. Earth Sci.* **1975**, *12*, 2080–2085. [CrossRef]
37. Irfan, T.Y. Mineralogy, fabric properties and classification of weathered granites in Hong Kong. *Q. J. Eng. Geol. Hydrogeol.* **1996**, *29*, 3–35. [CrossRef]
38. Ng, C.W.W.; Guan, P.; Shang, Y.J. Weathering mechanisms and indices of the igneous rocks of Hong Kong. *Q. J. Eng. Geol. Hydrogeol.* **2001**, *34*, 133–151. [CrossRef]
39. Guan, P.; Ng, C.W.W.; Sun, M.; Tang, W. Weathering indices for rhyolitic tuff and granite in Hong Kong. *Eng. Geol.* **2001**, *59*, 147–159. [CrossRef]
40. Chiu, C.F.; Ng, C.W.W. Relationship between chemical weathering indices and physical and mechanical properties of decomposed granite. *Eng. Geol.* **2014**, *179*, 76–89. [CrossRef]
41. Arel, E.; Tugrul, A. Weathering and its relation to geochemical properties of Cavusbasi granitic rocks in northwestern Turkey. *Bull. Eng. Geol. Environ.* **2001**, *60*, 123–133.
42. Kim, S.; Park, H.D. The relationship between physical and chemical weathering indices of granites around Seoul, Korea. *Bull. Eng. Geol. Environ.* **2003**, *62*, 207–212. [CrossRef]
43. Esaki, T.; Jiang, K. Comprehensive study of the weathered condition of 10 welded tuff from a historic stone bridge in Kagoshima, Japan. *Eng. Geol.* **2000**, *55*, 121–130. [CrossRef]
44. Jayawardena, U.S.; Izawa, E. Application of present indices of chemical weathering for Precambrian metamorphic rocks in Sri Lanka. *Bull. Eng. Geol. Environ.* **1994**, *49*, 55–61. [CrossRef]
45. Lee, C.H.; Yi, J.E. Weathering damage evaluation of rock properties in the Bunhwangsa temple stone pagoda, Gyeongju, Republic of Korea. *Environ. Geol.* **2007**, *52*, 1193–1205. [CrossRef]
46. Lee, D.S.; Lee, C.H.; Kim, J.; Yang, H.J. Geochemical characteristics of surface efflorescence on the seventh century stone pagoda in Republic of Korea. *Environ. Geol.* **2009**, *58*, 197–204. [CrossRef]
47. Ohta, T.; Arai, H. Statistical empirical index of chemical weathering in igneous rocks: A new tool for evaluating the degree of weathering. *Chem. Geol.* **2007**, *240*, 280–297. [CrossRef]
48. Arnold, A.; Zehnder, K. *Monitoring Wall Paintings Affected by Soluble Salts: The Conservation of Wall Paintings*; Cather, S., Ed.; Getty Conservation Institute: Marina del Rey, CA, USA, 1991; pp. 103–135.
49. Thomas, M.F. *Tropical Geomorphology*; Macmillan Press LTD: London, UK, 1974; 332p.
50. Charola, A.E. Salts in the deterioration of porous materials: An overview. *J. Am. Inst. Conserv.* **2000**, *39*, 327–343. [CrossRef]
51. Rodriguez-Navarro, C.; Doehne, E. Salt weathering: Influence of evaporation rate, supersaturation and crystallization pattern. *Earth Surf. Process. Landf. J. Br. Geomorphol. Res. Group* **1999**, *24*, 191–209. [CrossRef]